

# Peptide–protein interactions studied by surface plasmon and nuclear magnetic resonances

Ottavia Spiga<sup>a</sup>, Andrea Bernini<sup>a</sup>, Maria Scarselli<sup>a</sup>, Arianna Ciutti<sup>a</sup>, Luisa Bracci<sup>a</sup>,  
Luisa Lozzi<sup>a</sup>, Barbara Lelli<sup>a</sup>, Daniela Di Maro<sup>b</sup>, Duccio Calamandrei<sup>b</sup>, Neri Niccolai<sup>a,\*</sup>

<sup>a</sup>Biomolecular Structure Research Center and Department of Molecular Biology, University of Siena, via Fiorentina 1, I-53100 Siena, Italy

<sup>b</sup>BIOMODEM pscrl, via Fiorentina 1, I-53100 Siena, Italy

Received 15 November 2001; revised 29 November 2001; accepted 29 November 2001

First published online 19 December 2001

Edited by Thomas L. James

**Abstract** The structural features of the complexes that  $\alpha$ -bungarotoxin forms with three different synthetic peptides, mimotopes of the nicotinic acetylcholine receptor binding site, have been compared to the corresponding nuclear magnetic resonance (NMR) and surface plasmon resonance (SPR) data. For the considered peptides, the observed different affinities towards the toxin could not be accounted simply by static structural considerations. A combined analysis of the SPR- and NMR-derived dynamic parameters shows new correlations between complex formation and dissociation and the overall pattern of intramolecular and intermolecular nuclear Overhauser effects. These features could be crucial for a rational design of protein ligands. © 2002 Federation of European Biochemical Societies. Published by Elsevier Science B.V. All rights reserved.

**Key words:** Peptide–protein affinity; Protein complex; Ligand design; Intermolecular nuclear Overhauser effects; Nuclear magnetic resonance; Surface plasmon resonance

## 1. Introduction

Peptide and antigen fragment libraries obtained by the phage display technology have been extensively used to study antibody–antigen interaction in order to develop vaccines and diagnostic tools. Moreover, the same technology has been proposed, in general, for investigating any protein–protein or peptide–protein interaction for the design of selective ligands of potential pharmaceutical interest [1].

Understanding the fine details of these intermolecular processes is crucial to design peptide ligands with improved affinity and activity. In this respect, it is now well established that surface plasmon resonance (SPR) and nuclear magnetic resonance (NMR) are playing a major role in elucidating dynamics and structural aspects of protein–protein and peptide–protein complex formation. SPR yields accurate estimates of kinetic parameters of the intermolecular interaction, such as  $k_{\text{on}}$  and  $k_{\text{off}}$ , while NMR offers precious information on the

structural stability of the complex by analyzing intramolecular and intermolecular nuclear Overhauser effects (NOEs).

A strong correlation between the structure stability and the affinity between protein subdomains has been found from SPR data [2] and a combined use of SPR and NMR measurements has been proposed for investigating peptide–antibody [3,4] and virus–receptor interactions [5].

Among the various peptide–protein interactions, the complex formation between acetylcholine receptor (AChR) mimotopes and  $\alpha$ -bungarotoxin ( $\alpha$ -btx) has been analyzed in detail both by SPR [6] and NMR [7,8,9]. Thus, the structure of three slightly different complexes are available in the Protein Data Bank (PDB) with the 1JBD, 1HAA and 2BTX codes [10], where  $\alpha$ -btx is bound respectively to the peptides WRYESSLKPYPD, HRYESSLEPWYPD and MRYESSLKSYPD, henceforth called HaPep, p6.7 and LLPep. In the present report the favorable opportunity to discuss a good wealth of dynamic and structural data for such similar molecular systems will be exploited in order to correlate complex affinity with structural features. A good agreement of SPR derived  $K_A$  values with  $IC_{50}$  and  $K_A$  conventional methods has been recently discussed for the investigated system [6]. The SPR characteristics of these mimotopes and of some of their analogs will be also analyzed.

## 2. Materials and methods

The structural analysis of all the peptide–protein complexes was carried out on the basis of the 3D models generated with the program MOLMOL [11] for the corresponding PDB files 1JBD, 1HAA and 2BTX. Molecular volumes and exposed surfaces were calculated according to the Richards' algorithm [12] with a probe radius of 1.4 Å.

Peptides were synthesized on Rink Amide MBHA resin (Nova Biochem) using 9-fluorenylmethoxycarbonyl chemistry on an automated synthesizer (MutysynTech Syro); peptides were purified by high pressure liquid chromatography and identity and purity of final products was confirmed by electrospray ionization and matrix-assisted laser desorption ionization mass spectrometry.

SPR measurements were performed on a BIACORE 1000 Upgraded (BIACORE AB, Uppsala, Sweden). Biotin-conjugated  $\alpha$ -btx was immobilized on a streptavidin-coated sensor chip by injecting the toxin diluted in HEPES buffer saline (10 mM HEPES, 150 mM NaCl, 3.4 mM EDTA, 0.005% polysorbate 20, pH 7.4) (HBS; Biacore AB) at a concentration of 10  $\mu\text{g/ml}$  at a flow rate of 10  $\mu\text{l/min}$ . For kinetic experiments, peptides diluted in HBS at concentrations ranging from 6.5 to 0.06  $\mu\text{M}$  were injected at a flow rate of 30  $\mu\text{l/min}$  over the immobilized  $\alpha$ -btx.

Association and dissociation kinetic rate constants ( $k_{\text{on}}$  and  $k_{\text{off}}$ ) and the equilibrium association constant  $K_A$  were calculated using the BIAevaluation 3.0 software [13].

\*Corresponding author. Fax: (39)-577-234903.

E-mail address: niccolai@unisi.it (N. Niccolai).

**Abbreviations:** AChR, acetylcholine receptor; HaPep, WRYESSLEPYPD; LLPep, MRYESSLKSYPD; NMR, nuclear magnetic resonance; NOE, nuclear Overhauser effect; p6.7, HRYESSLEPWYPD; SPR, surface plasmon resonance;  $\alpha$ -btx,  $\alpha$ -bungarotoxin

### 3. Results and discussion

A SPR analysis of  $\alpha$ -btx binding kinetics has been performed on a series of AChR peptide mimotopes in identical experimental conditions (Fig. 1).

It is of primary interest the fact that the mimotope HaPep, which has the highest biological activity in terms of  $IC_{50}$  [9], experiences also the largest  $K_A$  value, deriving mostly from its very slow dissociation rate, see Fig. 1A. For p6.7 and HaPep, indeed, similar  $k_{on}$  rates were measured, suggesting that the higher affinity constant obtained for the latter mimotope can be totally ascribed to the stability of the complex.

The peptide–protein association process, quantitatively measured from SPR-derived  $k_{on}$  data, has been analyzed also with the aid of a series of p6.7 analogs. The N-terminus acetylated derivative of p6.7, acHRYESSLEPWYP, together with a series of its analogs, progressively shortened at the C-terminus up to a four-residue length, were analyzed in BIACORE (Fig. 1B). The corresponding  $k_{on}$  and  $k_{off}$  values are reported in the same figure.

Three main features appear from these SPR data: (i) no binding can be detected for peptides shorter than 11 residues, (ii) the acetylation of the amino terminus determines a four-fold reduction of the p6.7 rate, and (iii) within all the p6.7 analogs there is only a two-fold increase in the dissociation rates and more than one order of magnitude in the association decrease. The large observed changes in the association process can be attributed to two distinct aspects. The first one is related to the disappearance of the positive charge at the amino terminus, due to its acetylation, and to the removal of the hydrogen bond between  $^{H1}NH^{D14}O\delta_{p6.7}$  observed in the  $\alpha$ -btx/p6.7 complex structure [7]. This hypothesis suggests that this molecular moiety could act as an anchor towards the toxin binding site.

The second contribution to the observed association decrease may be determined by a reduced efficiency of the prolyl residue in position 10 as a folding inducer [7]. This explanation is also consistent with the fact that the shorter is the number of residues following this proline, the higher is its flexibility. In this case, it is apparent that the capability of this residue to induce the folding of the remaining part of the peptide chain is reduced.

Some of the NMR-derived structural features, available for  $\alpha$ -btx complexed with AChR mimotopes, are summarized in Table 1.

Table 1

Backbone heavy atoms RMSD calculated from the structure of the free  $\alpha$ -btx (PDB code 1IK8); numbers in parentheses refer to the considered fragments

	1JBD	1HAA	2BTX	1IK8
RMSD finger I (5–12)	1.55	1.41	1.91	–
RMSD finger II (28–39)	1.65	2.41	1.63	–
RMSD finger III (50–60)	2.97	2.07	2.61	–
RMSD carboxy terminus (70–74)	2.17	1.06	1.90	–
ESA ( $\text{\AA}^2$ )	4921	4994	4970	4432
Protein–peptide contact area ( $\text{\AA}^2$ )	742	606	502	–
Complex volume ( $\text{\AA}^3$ )	10025	11002	10863	–
$\alpha$ -btx volume ( $\text{\AA}^3$ )	9406	9113	9020	8729
Peptide volume in the complex ( $\text{\AA}^3$ )	1937	1878	1761	–
# long range intraprotein NOEs	759	245	291	368
# long range intrapeptide NOEs	27	12	7	–
# intermolecular NOEs	57	92	62	–

1JBD, 1HAA, 2BTX and 1IK8 are the PDB codes respectively of  $\alpha$ -btx/p6.7,  $\alpha$ -btx/HaPep,  $\alpha$ -btx/LLPep complexes and of  $\alpha$ -btx alone. The numbers of the observed NOEs are taken from the corresponding references (see text).

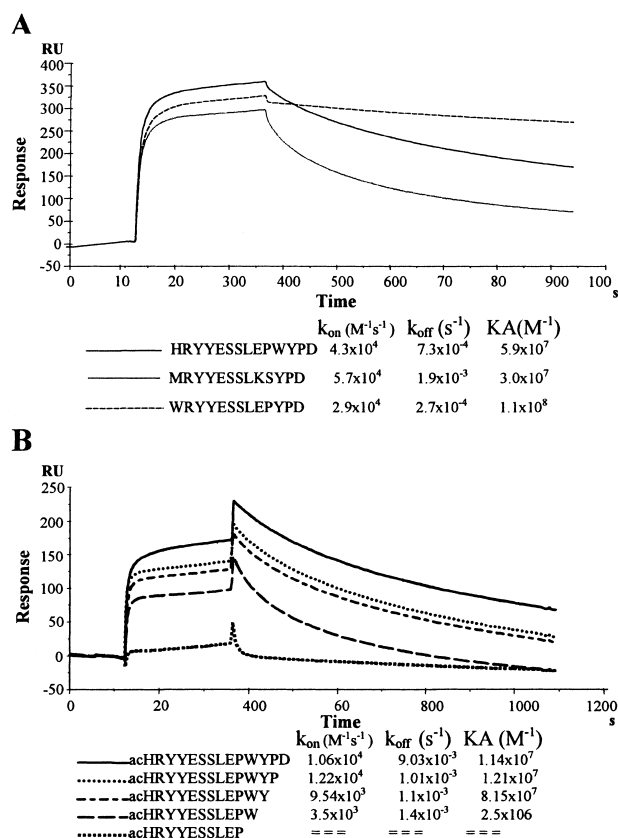


Fig. 1. A: SPR analysis of binding of peptide mimotopes p6.7, LLPep and HaPep to  $\alpha$ -btx. RU: Resonance unit. B: SPR analysis of binding of progressively shortened derivatives of p6.7 to  $\alpha$ -btx. Peptides were injected over a BIACORE SA sensor chip where biotinylated  $\alpha$ -btx had been previously captured via streptavidin.

From the PDB entries 1JBD, 1HAA and 2BTX, which refer to the average minimized structures of  $\alpha$ -btx respectively complexed with p6.7, HaPep and LLPep, rather different structural features can be observed, in spite of the close similarity in the mimotope lengths and amino acid compositions. The fact that, among the above mentioned structures, the  $\alpha$ -btx/p6.7 complex has the smallest volume and exposed surface area (ESA) suggests that this complex has the most compact conformation, also considering that p6.7 is one amino acid longer than the other two mimotopes. This compactness, reducing backbone flexibility, is fully consistent with the large

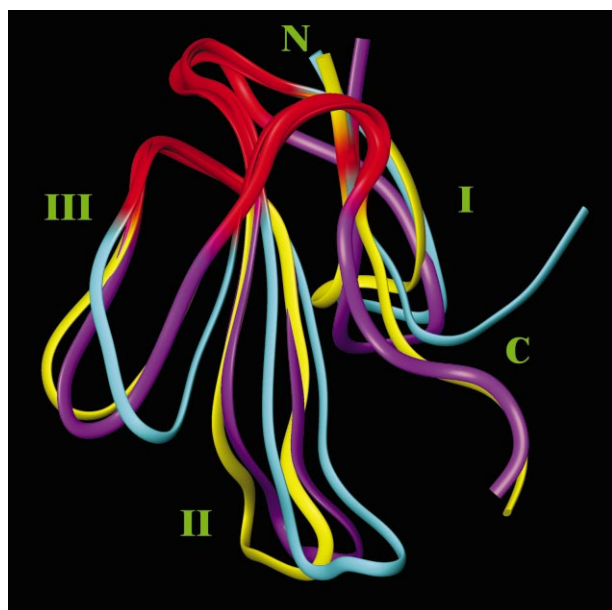


Fig. 2. Superposition of minimized average structures of  $\alpha$ -btX bound to three different AChR mimotopes (not shown). Toxin backbones of the complexes with p6.7, HaPep and LLPep are colored respectively in purple, cyan and yellow; red-colored backbone regions correspond to the aligned regions with the residues 3, 16–23, 44–48 and 59–65.

number of intramolecular NOEs detected for the peptide and protein moieties in the  $\alpha$ -btX/p6.7 complex.

Moreover, the calculated contact area between the toxin and the mimotope in the  $\alpha$ -btX/p6.7 complex results to be larger than in the other two cases.

Thus, peptide–protein contact areas, ESAs, volumes and number of intramolecular NOEs obtained for the three considered complexes seemed to predict a higher affinity of p6.7 towards  $\alpha$ -btX in respect to the other two mimotopes.

This hypothesis is fully discarded in light of the above discussed SPR results. It follows that complex stability, at least for this molecular system, but very likely in general, is influenced not only by steric contributions, but also by dynamic aspects.

The lowest  $k_{\text{off}}$  value observed for  $\alpha$ -btX/HaPep, a measure of the molecular compatibility between the protein and the peptide, is fully in agreement with the observation that the largest number of intermolecular NOEs is found, by far, for this complex.

Such a combined analysis of the SPR and NMR data offers interesting correlations, never discussed so far on the basis of experimental data, between  $k_{\text{off}}$  values and number of intermolecular NOEs, which seem to be precious to define further details of the peptide–protein interaction process.

The fact that a reliable solution structure of the free  $\alpha$ -btX is now available [7] allows new correlations between toxin structural changes, induced by the complexation with the three similar mimotopes, and the extent of the observed  $k_{\text{off}}$  values. A schematic view of  $\alpha$ -btX conformational rearrangements upon mimotope binding is given in Fig. 2. The toxin conformational change can be quantitatively described by a RMSD analysis of the positional parameters of the backbone heavy atoms in the critical regions of the toxin in the presence and in the absence of the complexed peptides. From the RMSD val-

ues reported in Table 1, it appears that the smallest conformational changes in the toxin fingers I and III and in the carboxy terminus backbone heavy atoms are induced by the HaPep complex formation. In this case, therefore, a smaller energy is required by  $\alpha$ -btX to accommodate HaPep rather than p6.7 and LLPep. It should be noted also that in the case of  $\alpha$ -btX/HaPep, exhibiting the highest RMSD for finger II, the required energy for these extensive conformational changes may be well counterbalanced by a favorable elongation of the toxin finger II  $\beta$ -sheet structure, which involves four additional residues.

It can be concluded that, at least in the case of the considered  $\alpha$ -btX–mimotope interactions, the complex stability cannot be fully explained in terms of molecular compactness or number of van der Waals and H bonding interactions.

From the analysis of the toxin conformational changes of the three complexes and the corresponding kinetic parameters, it can be suggested that entropic contributions may play a relevant role. The reduced conformational freedom observed for the  $\alpha$ -btX carboxy terminus, when bound to LLPep and p6.7 in respect to HaPep, seems to yield also a relevant contribution of this type.

Thus, it is apparent that the here proposed SPR/NMR combined approach offers new possibilities to investigate fine details of the peptide–protein interaction. These findings can be exploited to design ligands with improved affinity by means of amino acid substitutions, which can be suggested by the specific roles exhibited by each residue separately in association and dissociation processes.

Affinity maturation of ligands, derived from peptide libraries, on a rational structural and kinetic basis appears the main application of our approach.

**Acknowledgements:** Thanks are due to the Italian Ministry of University, Research and Technology (PRIN 1999) and to the University of Siena for financial support. Michela Bernardini is also acknowledged for helpful discussions.

## References

- [1] Sidhu, S.S. (2000) *Curr. Opin. Biotechnol.* 11, 610–616.
- [2] Berggard, T., Julenius, K., Ogard, A., Drakenberg, T. and Linse, S. (2001) *Biochemistry* 40, 1257–1264.
- [3] Phan-Chan-Du, A., Petit, M.C., Guichard, G., Briand, J.P., Muller, S. and Cung, M.T. (2001) *Biochemistry* 40, 5720–5727.
- [4] Wu, G. (2000) *J. Biol. Chem.* 275, 36645–36652.
- [5] Urban, S., Schwarz, C., Marx, U.C. and Multhaup, G. (2000) *EMBO J.* 19, 1217–1227.
- [6] Bracci, L., Lozzi, L., Lelli, B., Pini, A. and Neri, P. (2001) *Biochemistry* 40, 6611–6619.
- [7] Scarselli, M., Spiga, O., Ciutti, A., Bernini, A., Bracci, L., Lelli, B., Lozzi, L., Calamandrei, D., Di Maro, D., Klein, S., Niccolai, N. (2002) *Biochemistry*, in press.
- [8] Scherf, T., Balass, M., Fuchs, S., Katchalski-Katzir, E. and Anglister, J. (1997) *Proc. Natl. Acad. Sci. USA* 94, 6059–6064.
- [9] Scherf, T., Kasher, R., Balass, M., Fridkin, M., Fuchs, S. and Katchalski-Katzir, E. (2001) *Proc. Natl. Acad. Sci. USA* 98, 6629–6634.
- [10] Berman, H.M., Westbrook, J., Feng, Z., Gilliland, G., Bhat, T.N., Weissig, H., Shindyalov, I.N. and Bourne, P.E. (2000) *Nucleic Acids Res.* 28, 235–242.
- [11] Koradi, R., Billeter, M. and Wüthrich, K. (1996) *J. Mol. Graph.* 14, 29–32.
- [12] Richards, F.M. (1985) *Methods Enzymol.* 115, 440–464.
- [13] Karlsson, R. and Fält, A. (1997) *J. Immunol. Methods* 200, 121–133.